Enhancing of Features for Road Crack Image Using EEcGANs

Amal Mohammed Jaber and Farah Abbas Obaid Sari*

Computer Science, Faculty of Computer Science and Mathematics, University of Kufa, Najaf, Iraq

Email: amalm.alkreiti@student.uokufa.edu.iq (A.M.J.), faraha.altaee@uokufa.edu.iq (F.A.O.S.)

Abstract—**Continuously monitoring roads to examine their defects is a difficult task for the human element due to the increasing length of roads. Therefore, several types of digital imaging tools are used, for example (drones, surveillance cameras fixed on poles and cameras fixed on a moving car). These imaging tools automatically take pictures under various weather conditions and the blurriness generated by cameras mounted on moving cars. This paper proposes a method to enhance road surface images captured under different conditions, where the image will be improved in the frequency domain and spatial domain and then added to the enhancement with the Enlighten of Conditional Generative Adversarial Networks (EEcGANs) to obtain a generated and enhanced image. The metrics Peak Signal-to-Noise Ratio (PSNR), Structural Similarity Index (SSIM), Difference in Variance (DIV), Correlation Coefficient (CC) and Universal Quality Index (UIQ) are used to evaluate the performance of the proposed method, achieving the values 29.4019, 0.8996, − 0.12151, 972758 and 0.970491, respectively.**

Index Terms—**Conditional Generative Adversarial Networks (cGANs), evaluation metrics for the generated image, image enhancements methods, N-RDD2024 dataset**

I. INTRODUCTION

In countries with snow, dust and fog, harsh environmental conditions obstruct capturing high-quality images. Photos taken even in unstable weather conditions often hide many details in the images, especially those that contain fine details such as road defects. However, environmental factors and camera constraints in such situations have rendered quality imaging for accurate road defect identification impossible [1–3]. The color and noise are seriously damaged in the captured images, while there is also uneven brightness, artefacts and many other problems. Fig. 1 shows degraded images in different weather conditions from a few countries.

Traditional image processing algorithms are often unsatisfactory for solving the problem of detecting foreign objects in images taken in bad weather. They are, therefore, not suitable for solving vision tasks that require preserving information without distortion or exaggeration.

This requires image enhancement techniques specialized in road defect detection and classification applications.

We can spot right away that the fundamental problems of image enhancement that need to be solved are noise and blur and dark areas covering major parts due to darkness, light attenuation or scattering. This phenomenon reduces the color intensity and saturation levels and decreases the brightness of specific colors to represent image. On the other hand, image distortion in photography, whether using regular cameras or surveillance, occurs primarily due to clouds and dust blocking light. Such influences lead to a gradual loss in concordance and resolution of images, compromising the fidelity and the precision of the visual outputs. However, only considering these aspects is insufficient to produce a better image enhancement effect in the most adverse shooting conditions. These are much more challenging conditions for algorithms to generalize and recover features well.

Fig. 1. Degraded images in different weather conditions.

Based on this analysis and given these challenges, in this paper, we propose an EEcGANs method to reconstruct and enhance road defect images to enhance the feature detection and selection process. The features enhanced using the proposed algorithm can and will inevitably improve the accuracy of machine learning algorithms and help them detect road defects [4].

II. LITERATURE REVIEW

Image processing methods are still developing, and their applications have become widespread and indispensable, prompting many researchers to expand in this field. Previous works focus on processing infrastructure images, including road surface defects, to improve the economic level of developing and developed countries. We will

discuss some interesting previous works and analyze them later.

Salimans *et al*. [5] introduced various novel architectural elements and training procedures applied to the generative adversarial networks (GANs) framework. Activate MNIST, CIFAR-10 and SVHN with state of art semi-supervised classification methods error to obtain an error rate of 21.3%.

Zhang *et al*. [6] used an adversarial learning method to enhance underwater photographs. Preprocessing is first used to solve the dataset's severe color casting. Then, to restore the network output's features more effectively, relevant enhancements are made to the loss functions and structural design of generative adversarial networks. The performance of this work was evaluated with 22.467 PSNR.

Maeda *et al*. [7] enhanced the road damage identification accuracy by using a Poisson blending algorithm with a progressive growing GAN to create artificially generated road damage images that can be utilized as fresh training data. For modest and relatively large numbers of original photos, respectively, adding a synthesized image of road damage to the training data increases the F-measure by 5% and 2%.

Yan *et al*. [8] suggested a low-light image-enhancing technique based on GAN with improved network module optimization. The proposed method first input the image into the generator to create a similar image in the new space. Next, it constructed and minimized a loss function to train the discriminator, which compares the image produced by the generator with the original image. The proposed method was implemented on two image datasets (DPED, LOL) to compare with the deep learning approach and the conventional picture enhancement method. The GAN with improved network module optimization rose by 34.8% and 23.39% on SSIM-GC and by 69.56% and 43.06% on PSNR and SSIM-GC, respectively, according to experiments. In comparison to the existing deep learning techniques, a deep-stacked Laplacian restorer (DSLR), and Enlighten GAN, we also saw improvements in PSNR of 0.20% and 1.3%, SSIM of 0.29% and 23.23%, and SSIM-GC of 20.67% and 1.23%, respectively.

Li *et al*. [9] offered a learning technique to improve low-intensity images. This learning improves low-light images using conditional GANs. Specifically, they built an effective low light-enhancement model based on GAN loss, perceptual loss and structural similarity loss using a convolutional neural network with residual structures as generator and WGAN-GP as discriminator. The research uses PSNR=18.67 and SSIM=0.79 as their main evaluation metrics.

Salaudeen and Çelebi [10] employed super-resolution generative adversarial networks (GAN), such as enhanced super-resolution generative adversarial networks (ESRGAN), to improve the image quality of road surfaces, and used different object detection networks in the same pipeline to detect instances of potholes in the images. The architecture of the proposed method in this study consisted of two main components: ESRGAN and a detection network. The detection network used both you only look once (YOLOv5) and efficient detection networks. Yielding a precision value of 89.9.

Jia *et al*. [11] proposed a cycle-consistent generative adversarial network to improve the quality of nighttime road scene images, where the architecture of this network consisted of two generative networks and two adversarial networks with the same structures. The generative network consisted of an encoder network and a matching decoder network. The underlying design of the encoder-decoder network was context feature extraction modules to identify richer contextual semantic information under a broader spatial range. The approaches presented in the research mainly utilize PSNR=28.63 and SSIM=0.86 as the evaluation criteria.

III. PROPOSED METHOD

In this paper, enhancing road surface images includes two stages. The first stage will consist of a preprocessing process for the image in (spatial and frequency domain) [12, 13], while the second stage will include building a network (EEcGANs)to enhance the image.

A. Dataset

First, let us talk about the old version of the road damage dataset. RDD2022 (road damage dataset) contains 47,420 road images from almost six countries, including Japan, India, the Czech Republic, Norway, the United States, and China. The dataset contains more than 55000 records of road damage, such as longitudinal cracks, transverse cracks, alligator cracks, and potholes. The RDD2024 dataset contains road images from the six countries mentioned above. However, 10 different types of defects were considered in the presented dataset. The images of this dataset were taken in various weather conditions depending on the kind of weather in that country. For example, the images of Norway contain snow, the images of India contain heavy dust, and the images contain fog in the United States [14].

B. Preprocessing Degraded Image of Surface Roads

The difference in the shapes and sizes of road defects due to weather deterioration in some countries prevents neural networks from distinguishing these cracks and holes and increases the difficulty of detecting them. At this stage, the road surface images will be processed, improving the image's density value, and increasing the number of features the network EEcGANs will acquire, as shown in Fig. 2.
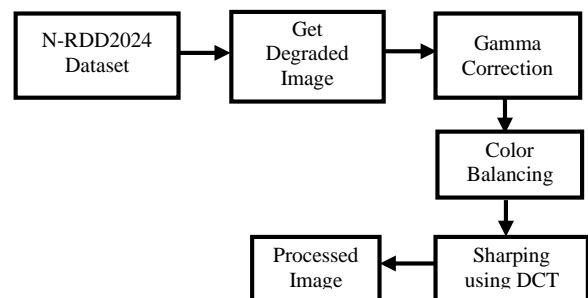

Fig. 2. Block diagram of preprocessing.

Three levels of pre-enhancement will be used, as follows:

1) Gamma correction

The gamma factor, or simply gamma, defines the relationship between the numerical value of a pixel and its actual luminosity. Without gamma correction, dark tones captured by digital cameras would not look the way our eyes see them [15]. In this case, gamma converts the camera's readings to our eyes' sensitivity. When a digital image is saved, it is gamma-encoded so that a doubling of the value in the file more closely corresponds to what we perceive as a doubling of the brightness. The most commonly used transfer function for gamma correction is a power function as in (1):

$$V_{out} = AV_{in}^{\gamma} \quad (1)$$

where A serves as a coefficient, γ represents the gamma parameter, and the input V_{out} and output V_{in} values are non-negative real numbers.

In general, if $A=1$, the input and output values range from 0 to 1. When gamma is equal to one, the halftone transfer characteristic is linear, and the differences in the illumination of the object in the highlights and shadows are displayed equally.

2) Color balancing

The goal of color balancing is color constancy by removing the effects of illumination on all colors, since in the balancing process colors other than white are not considered to convert the white point to a ground truth one. To handle this problem, Cheng *et al.* proposed a method to reduce lighting effects on all colors under the framework of white balancing [16].

Let

$$\mathbf{T}_1' = \left(X_{T_1}', Y_{T_1}', Z_{T_1}'\right), \mathbf{T}_2' = \left(X_{T_2}', Y_{T_2}', Z_{T_2}'\right),$$

$$\mathbf{T}_3' = \left(X_{T_3}', Y_{T_3}', Z_{T_3}'\right), \ \mathbf{T}_n' = \left(X_{T_n}', Y_{T_n}', Z_{T_n}'\right)$$

be n target colors with remaining lighting effects in the *XYZ* color space. And let

$$\mathbf{G}_1' = \left(X_{G_1}', Y_{G_1}', Z_{G_1}'\right), \ \mathbf{G}_2' = \left(X_{G_2}', Y_{G_2}', Z_{G_2}'\right)$$

$$\mathbf{G}_3' = \left(X_{G_3}', Y_{G_3}', Z_{G_3}'\right), \qquad \mathbf{G}_n' = \left(X_{G_n}', Y_{G_n}', Z_{G_n}'\right)$$

be n ground truth colors corresponding to each target color

To calculate the linear transform matrix of $\mathbf{T}'$ and $\mathbf{G}'$ as in (2) and (3) respectively:

$$\mathbf{T}' = \begin{pmatrix} X_{T_1}' & X_{T_2}' & X_{T_3}' & & X_{T_n}' \\ Y_{T_1}' & Y_{T_1}' & Y_{T_3}' & \cdots & Y_{T_n}' \\ Z_{T_1}' & Z_{T_2}' & Z_{T_2}' & & Z_{T_n}' \end{pmatrix} \quad (2)$$

$$\mathbf{G}' = \begin{pmatrix} X_{G_1}' & X_{G_2}' & X_{G_3}' & & X_{G_n}' \\ Y_{G_1}' & Y_{G_2}' & Y_{G_3}' & \cdots & Y_{G_n}' \\ Z_{G_1}' & Z_{G_2}' & Z_{G_3}' & & Z_{G_n}' \end{pmatrix} \quad (3)$$

Cheng's method assumes $n=24$.

3) Sharpening degraded image using discrete Fourier transform (DCT) [17]

The things that are of interest when enhancing road surface images are cracks and potholes, so the edges of these cracks and potholes will be the focus of attention.

Image sharpening is used to highlight the cracks' edges and increase the enhancement's accuracy and response speed. The enhancement will be in the frequency mode by transforming the image from spatial to the frequency domain as in (4). The conversion to the spatial domain is done when the image processing is complete using DCT^{-1} as in (5).

$$H(u,v) = c(u)c(v)\sum_{x=0}^{N-1}\sum_{y=0}^{M-1} f(x,y)\cos\left(\frac{\pi u(2x+1)}{2N}\right)\cos\left(\frac{\pi v(2y+1)}{2M}\right) \quad (4)$$

$$F(x,y) = c(u)c(v)\sum_{u=0}^{N-1}\sum_{v=0}^{M-1} f(u,v)\cos\left(\frac{\pi u(2x+1)}{2N}\right)\cos\left(\frac{\pi v(2y+1)}{2M}\right) \quad (5)$$

where x and y represent two dimensions of the image associated with spatial domain, u and v represent two dimensions of the image related to the frequency domain, $H(u, v)$ is the DCT transform, and $F(x, y)$ stands for pixel values of the image in the spatial domain, M and N are the dimensions size of the image in the spatial domain, and $c(u)$, $c(v)$: The compensation coefficients that establish the orthogonality of the DCT-transformation matrix and can be calculated as in (6) and (7) respectively:

$$c(u) = \begin{cases} \sqrt{\frac{1}{N}}, & u = 0 \\ \sqrt{\frac{2}{N}}, & u \neq 0 \end{cases} \quad (6)$$

$$c(v) = \begin{cases} \sqrt{\frac{1}{M}}, & v = 0 \\ \sqrt{\frac{2}{M}}, & v \neq 0 \end{cases} \quad (7)$$

Sharpening images passing the high frequencies blocks the low as in (8):

$$H(u,v) = \frac{1}{2\pi\sigma^2}(1 - \ell^{-(u^2+v^2)/2\sigma^2}) \quad (8)$$

where σ^2 represent variance.

C. Enhancement with Enlighten of Conditional Generative Adversarial Networks (EEcGANs)

Image augmentation algorithms could greatly benefit from combining conditional generative adversarial networks (cGANs) with Enlighten GAN, which is a promising way of further extending their capabilities.

When processing low-light images using cGANs, you could condition the model on metadata such as the type of scene (indoors, outdoors, etc.) or the desired enhancement technique. The convergence can employ conditional inputs to regulate which image areas require enhancement to benefit from enlighten GAN's low-light design. For instance, several augmentation techniques can be used

depending on the conditional labels.

The proposed algorithm EEcGANs consists of a combination of Enlighten GAN [18] and conditional GAN, where complete architecture consists of two parts (generative and discriminative), as shown in Fig. 2 and Fig. 3. The generator network structure has nine residual blocks, two transposed convolution blocks, two convolution blocks with a step length of two, and deblurring. A convolution layer, an instance normalized layer, and a rectified linear activation function (RELU) with a learning rate=0.0002, Epochs=150, and Batch sizes=16 make up each residual block. Furthermore, the skip connection is added to preserve more original image features globally. Besides the output of cGANs, we propose adding the

enlighten block to produce 2 times upsampling results as support for the target.

Fig. 2 exhibits the architecture of the generative part, with recursive learning and residual learning to extract features and use extracted features to predict multi-level images. With the help of the Enlighten box, feature maps derived from the skip connection can learn high-frequency information in alternating easier and more challenging modes and gain relevant gradients.

Because of its multi-output architecture, it gives the network the ability to generalize more importance. As a result, the produced images are organic and realistic.
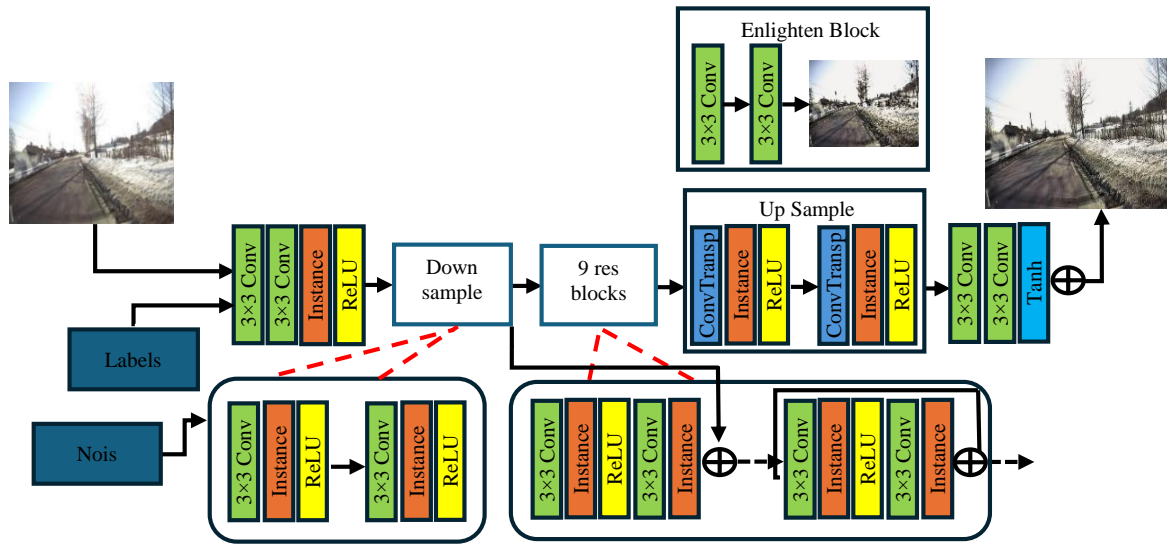
Fig. 2. Generative part of EEcGANs algorithm.
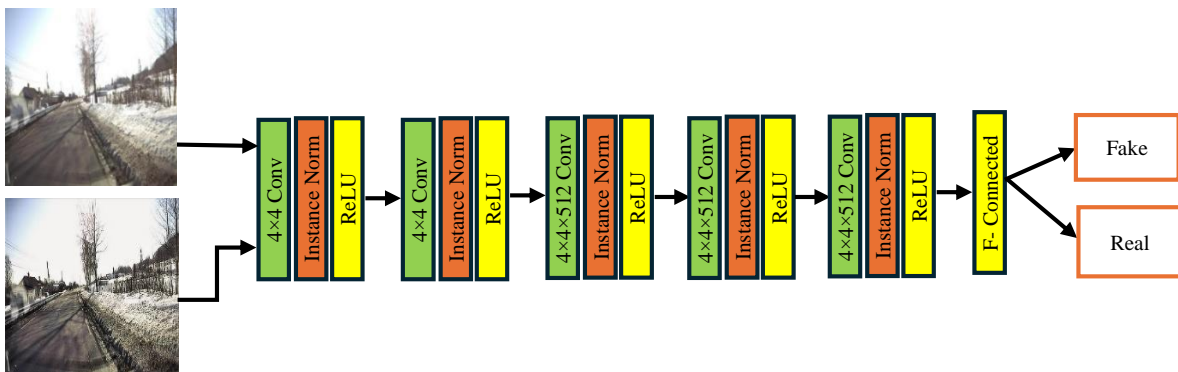
Fig. 3. Discriminative part of EEcGANs algorithm.

Fig. 3 shows how the discriminative part improves the quality of generated images by differentiating between authentic and fraudulent images and giving the generative network an adversarial loss. This part receives labels and generated images fed to convolution and batch normalization layers. At the end of this network discriminative, there are fully connected layers with soft max to predict the possibility of the given image being true.

IV. RESULTS ANALYSIS

Since this paper proposed a method to improve the

algorithm (cGANs), training and testing will focus on the dataset using the algorithms that make up the proposed method individually and the algorithm (EEcGANs). The training was done in five countries using a dataset containing diverse images based on the weather diversity in those countries. The images showed distinct clarity, as shown in Table I.
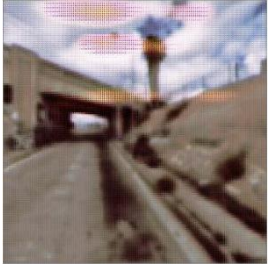
Several types of image quality metrics were used after improvement to measure the efficiency of the proposed algorithm compared to other sub-algorithms, as follows.

A. Peak Signal-to-Noise Ratio (PSNR)

This measure can be used as a metric for the quality of images generated from our proposed method, which can be considered the ratio of a signal's most significant value

(power) to the power of distorting noise that degrades the signal representation. The PSNR is typically stated using the logarithmic decibel scale because many signals have a wide dynamic range or the ratio of a variable quantity's highest and lowest possible values [19].

TABLE I: COMPARISON RESULTS BETWEEN GENERATED IMAGE FROM PROPOSED GAN AND OTHER GAN ALGORITHMS

Original Image	cGANs	Enlighten GANs	EEcGANs (Our)

PSNR can calculated as

$$\text{PSNR}_{(I,G)} = 20\log_{10}\left(\text{MAX}_h / \sqrt{\overline{\text{MSE}_{(I,G)}}}\right) \qquad (9)$$

where I is the original image, G represents the generated image from EEcGANs MSE (mean square error), h reflects our original image's matrix data, and MAX_h is the maximum signal value in our original image.

B. Structural Similarity Index (SSIM)

Proposed SSIM for test generated images based on measurement of similarity between two images, and can be calculated as in (10) [20, 21]:

$$\text{SSIM}_{(I,G)} = \frac{(2\mu_I\mu_G + c_1)(2\sigma_{I,G} + c_2)}{(\mu_I^2 + \mu_G^2 + c_1)(\sigma_I^2 + \sigma_G^2 + c_2)} \qquad (10)$$

where μ_I and μ_G represent mean values of original and generated images, respectively, and C_i Constants values.

C. Difference in Variance (DIV) [22]

A [Difference in Variance] >= 1 indicates a reasonably significant variance, while a DIV < 1 can be considered low. Accordingly, distributions with more than one coefficient of variation (DIV) are regarded as high variance, whereas those with a DIV of less than one are seen as having low variance.

This paper used metric DIV to calculate the difference in variance between the original image and the generated image using our proposed method as in (11).

$$\text{DIV}_{(I,G)} = 1 - \frac{\sigma_G^2}{\sigma_I^2} \qquad (11)$$

D. Correlation Coefficient (CC) [23]

A correlation coefficient quantifies the relationship between neighbouring pixels in an image. Higher encryption security is indicated by a lower correlation coefficient, which makes it more difficult to glean useful information from the picture. A value between -1.0 and 1.0 represents the correlation coefficient. The two photos' pixel values are the same when the correlation coefficient is 1.0. The two photos' pixel values are entirely out of sync when the correlation coefficient is -1.0 and can be found as in (12).

$$\text{CC}_{(I,G)} = \frac{\sigma_{(I,G)}}{\sigma_I \sigma_G} \qquad (12)$$

E. Universal Quality Index (UQI) [24]

Image distortion is modelled as a mixture of contrast, brightness distortion, and loss of correlation to produce the universal quality image index (UQI). The UQI ranges between 0 and 1. An image is considered good quality if its UQI is 1. A highly distorted image will have a low UQI, which can be calculated as in (13).

$$\text{UIQ}_{(I,G)} = \frac{4\sigma_{I,G}\overline{IG}}{(\sigma_I^2 + \sigma_G^2)(\overline{I}^2 + \overline{G}^2)} \qquad (13)$$

The calculation most of metrics used σ as standard deviation, σ^2 as variance, I as the original image, G as the generated image, $\overline{I}$ is the average of grayscale for image I and $\overline{G}$ is the average of grayscale for image G. It was necessary to use the mentioned metrics on all images tested using different types of GAN to identify the efficiency of the proposed algorithm (EEcGANs), as in Table II.

TABLE II: COMPARISON OF QUALITY METRICS RESULTS BASED ON DIFFERENT TYPES OF GAN ALGORITHM

Method	PSNR	SSIM	DIV	CC	UQI
cGANs	18.907	0.491	−0.276	0.757	0.747
Enlighten GANs	8.800	0.529	0.709	0.927	0.740
EEcGANs	**29.401**	**0.896**	**−0.121**	**0.972**	**0.970**

Looking at Table II, we find that the values of the metrics are favourable for the proposed method, and there is an actual performance improvement in the proposed algorithm EEcGANs. Compared to previous works that share two metrics, which are PSNR and SSIM, we notice that the value of PSNR has increased significantly and

reached 29.4019, while for the metric SSIM it was also a positive increase and became 0.8996.

V. CONCLUSION

In this paper, the cGANs algorithm is combined with Enlighten GAN to form EEcGANs. In addition, image sharpening, contrast, and color balancing are used as preprocessing. It is worth mentioning that the hybrid algorithm formation focuses on highlighting defects in the roads and not increasing the image in general to support faster damage detection. Build a hybrid from the cGANs and Enlighten GANs and adapt the discriminator and generator parts. The generator can accept the additional features from Enlighten GANs and the conditional input from cGANs, allowing for generating conditionally regulated high-quality images. The discriminator determines whether the generated image is realistic and consistent with the conditional inputs, reinforcing this dual-sided evaluation of the generated outputs. However, the values of the used metrics proved the efficiency of the proposed method, as the value of PSNR= 29.4019 reached, SSIM= 0.8996, DIV=-0.12151, CC=0.972758 and UQI=0.970491. We can conclude that most metrics were not used in previous works. In addition, there were challenges during the training process, the most important of which was the road damage, as they were exact and challenging to focus on to improve their actual visibility in the image. We can conclude that most metrics were not used in previous works. In addition, there were challenges during the training process, the most important of which was the road damage, as they were exact and complex to focus on to improve their actual visibility in the image. The final results were very satisfactory, and the proposed algorithm achieved the paper's goal.

CONFLICT OF INTEREST

The authors declare no conflict of interest.

AUTHOR CONTRIBUTIONS

Author: Amal Mohammed Jaber, the principal writer who prepared all the articles, summarized all the data and made the articles easy to read. Guided the entire review process in terms of its scope and focus. Farah Abbas Obaid Sari audited and reported on relevant research articles. All authors had approved the final version.

REFERENCES

[1] D. Dong and Z. Li, "Smartphone sensing of road surface condition and defect detection," *Sensors*, vol. 21, no. 16, #5433, 2021.

[2] R. Chhabra, C. R. Krishna, and S. Verma, "A survey on state-of-the-art road surface monitoring techniques for intelligent transportation systems," *International Journal of Sensor Networks*,

vol. 37, no. 2, pp. 81–99, 2021.

[3] A. Vittorio, V. Rosolino, I. Terese *et al.*, "Automated sensing system for monitoring of road surface quality by mobile devices," *Procedia-Social and Behavioral Sciences*, vol. 111, pp. 242–251, 2014,

[4] P. Yu, K. Song, and J. Lu, "Generating adversarial examples with conditional generative adversarial net," in *Proc. of 2018 24th Int. Conf. on Pattern Recognition (ICPR)*, 2018, pp. 676–681.

[5] T. Salimans, I. Goodfellow, W. Zaremba *et al.*, "Improved techniques for training gans," *Advances in Neural Information Processing Systems*, vol. 29, 2016. doi: 10.48550/arXiv.1606.03498

[6] M. Zhang, Y. Li, and W. Yu, "Underwater image enhancement algorithm based on adversarial training," *Electronics*, vol. 13, no. 11, #2184, 2024.

[7] H. Maeda, T. Kashiyama, Y. Sekimoto *et al.*, "Generative adversarial network for road damage detection," *Computer-Aided Civil and Infrastructure Engineering*, vol. 36, no. 1, pp. 47–60, 2021.

[8] L. Yan, J.-R. Fu, C. Wang *et al.*, "Enhanced network optimized generative adversarial network for image enhancement," *Multimedia Tools and Applications*, vol. 80, pp. 14363–14381, 2021. https://doi.org/10.1007/s11042-020-10310-z

[9] H. Li, J. Cheng, T. Liu, B. Cheng, and Z. Liu, "Low-light image enhancement based on conditional generative adversarial network," *Journal of Physics: Conference Series*, vol. 2035, no. 1, #012027, 2021.

[10] H. Salaudeen and E. J. E. Çelebi, "Pothole detection using image enhancement GAN and object detection network," *Electronics*, vol. 11, no. 12, #1882, 2022.

[11] Y. Jia, W. Yu, G. Chen, and L. J. S. R. Zhao, "Nighttime road scene image enhancement based on cycle-consistent generative adversarial network," *Scientific Reports*, vol. 14, no. 1, #14375, 2024.

[12] Y. Guo, Y. Zhu, L. Liu, and H. Qiang, "Research review of space-frequency domain image enhancement methods," *Journal of Computer Engineering & Applications*, vol. 58, no. 11, #23, 2022.

[13] Z. He, W. Ren, S. Liu *et al.*, "Low-light image enhancement with multi-scale attention and frequency-domain optimization," *IEEE Trans. on Circuits and Systems for Video Technology*, vol. 34, no. 4, pp. 2861–2875, Apr. 2024.

[14] Ö. Ç. Kaya and M. Yasin, "N-RDD2024: Road damage and defects," *Mendeley Data*, vol. 3, 2024. doi: 10.17632/27c8pwsd6v.3

[15] M. Ju, C. Ding, Y. J. Guo *et al.*, "IDGCP: Image dehazing based on gamma correction prior," *IEEE Trans. on Image Processing*, vol. 29, pp. 3104–3118, Dec. 2019.

[16] D. Cheng, B. Price, S. Cohen, and M. S. Brown, "Beyond white: Ground truth colors for color constancy correction," in *Proc. of the IEEE Int. Conf. on Computer Vision*, 2015, pp. 298–306.

[17] A. M. John, K. Khanna, R. R. Prasad, and L. G. Pillai, "A review on application of fourier transform in image restoration," in *Proc. of 2020 Fourth Int. Conf. on IoT in Social, Mobile, Analytics and Cloud*, 2020, pp. 389–397.

[18] M. Panwar and S. B. C. Gaur, "Performance analysis of enlighten GAN on low-light enhancement and denoising," *Series B*, vol. 105, pp. 677–684, Feb. 2024.

[19] A. Horé and D. Ziou, "Is there a relationship between peak-signal-to-noise ratio and structural similarity index measure?" *IET Image Processing,* vol. 7, no. 1, pp. 12–24, 2013.

[20] J. Nilsson and T. Akenine-Möller, "Understanding ssim," *arXiv preprint,* arXiv:2006.13846, 2020.

[21] A. A. H. Alrammahi, F. A. O. Sari, and H. A. H. Shamsuldeen, "Analysis of the development of fruit trees diseases using modified analytical model of fuzzy c-means method," *Indonesian Journal of Electrical Engineering and Computer Science*, vol. 29, no. 1, pp. 358–364, 2023.

[22] Z.-P. Zhou and X.-X. Zhang, "Image splicing detection based on image quality and analysis of variance," in *Proc. of 2010 2nd Int. Conf. on Education Technology and Computer*, 2010, vol. 4, pp. V4-242–V4-246.

[23] D. Inamdar, G. Leblanc, R. J. Soffer, and M. Kalacska, "The correlation coefficient as a simple tool for the localization of errors in spectroscopic imaging data," *Remote Sensing*, vol. 10, no. 2, #231, 2018.

[24] F. P. Lestari, C. Anam, Y. Hardiyanti, and F. Haryanto, "Automated universal image quality index measurement vs. Automated noise measurement: Which method is better to define CT image quality?" *Jurnal Penelitian Fisika dan Aplikasinya (JPFA)*, vol. 9, no. 2, pp. 132–139, 2019.

Amal Mohammed Jaber earned a bachelor's degree in computer science from the University of Babylon in 2005. She is currently working as a master's degree student in graduate studies. Her research interests include deep learning and computer vision.

Farah Abbas Obaid Sari received her master degree in information technology from Dr. Babasaheb Ambedkar Marathwada University in Aurangabad, India, and Ph.D. degree in data mining from Tambov State Technical University, Russia, in 2022. Currently, he works at the University of Kufa in Najaf, Iraq. His research interests include Image processing and artificial intelligence.